

2D Numerical Simulation of Fluid Flow over a Rectangular Prism

Sumeet Thete¹, Kaustubh Bhat¹ and M. R. Nandgaonkar^{1c}

¹ Mechanical Engineering Department, College of Engineering, Pune, India

Received: 16/07/2009 – Revised 16/07/2009 – Accepted 29/07/2009

Abstract

This paper is a part of an elaborate research involving simulation and practical testing of flows across solid objects. The research presented here deals with only the numerical modelling of such flows by development of code specifically for this purpose. The objective of this paper is to model the unsteady flow of incompressible fluid across a rectangular prism using simple collocated grid arrangement for Navier-Stokes Equation. The flow has been modelled numerically and flow visualizations have been generated for increasing values of Reynolds Number for a fluid at high kinematic viscosity. These results have been validated against previously probed values of the Strouhal Number versus the Reynolds Number. Also, an investigation has been made into the flow characteristics of a fluid at low kinematic viscosity in comparison with the highly viscous fluid at the same Reynolds Number. The simulations have been performed at low values of Reynolds Number. A prism of unit depth was chosen. The numerical investigation provides substantial information regarding the vortex shedding characteristics with increasing values of Reynolds Number.

Keywords: *Navier-Stokes Equation; Reynolds Number; Strouhal Number; Rectangular Prism; Kinematic Viscosity*

1. Introduction

A lot of research has been conducted in evaluating flow properties across solid objects. The weak conservative Navier-Stokes (N-S) equation has been found to be useful in solving such problems for low Reynolds number (Re). Since the flow occurs at low values of Re , a 2D simulation is quite accurate.

The paper concerns with the modelling of such a flow across a solid obstruction, here, a rectangular prism using a simple collocated grid method for solving the N-S equations using a finite volume approach. Consequently, this paper aims at demonstrating the vortex characteristics with increasing Reynolds Number. To avoid pressure-velocity decoupling, the solution was evaluated under unknown pressure and velocity fields using a semi-explicit pressure correction approach [1].

^c Corresponding Author: M. R. Nandgaonkar
 Email: mrn@mech.coep.org.in Telephone: +9120 25507223
 © 2009-2012 All rights reserved. ISSR Journals

The fluid under consideration is constrained to be incompressible. Thus, the solution addresses primarily the flow of liquids across a solid obstruction. The solid is assumed to be fixed, i.e. at a zero velocity. Also, the solid is assumed to be strong enough to sustain the stresses induced on it and that the elastic deformation in the solid has no effect on the flow characteristics.

This problem is largely insolvable using an analytical approach, and this paper aims at presenting a very simple approach for modelling such flows. A similar approach was used by Sharma and Eswaran [2] and the results obtained here are found to be consistent. The problem is of special significance in certain heat transfer apparatus such as heat exchangers. It also helps in the study of boundary layer characteristics in such flows.

2. Numerical details

2.1. Governing equations [3]

The N-S Equation for compressible fluids in Cartesian co-ordinates is given by:

(a) Continuity:

$$\frac{\partial \rho}{\partial t} + \nabla \cdot (\rho \mathbf{V}) = 0 \quad (1)$$

(b) X-Momentum:

$$\frac{\partial(\rho u)}{\partial t} + \nabla \cdot (\rho u \mathbf{V}) = -\frac{\partial p}{\partial x} + \frac{\partial \sigma_{xx}}{\partial x} + \frac{\partial \tau_{yx}}{\partial y} \quad (2)$$

(c) Y-Momentum:

$$\frac{\partial(\rho v)}{\partial t} + \nabla \cdot (\rho v \mathbf{V}) = -\frac{\partial p}{\partial y} + \frac{\partial \sigma_{yy}}{\partial y} + \frac{\partial \tau_{xy}}{\partial x} \quad (3)$$

For an incompressible flow, the equations can be generalised by eliminating the density term. Finite Volume discretization of these equations yields the following general equation

$$\rho \Delta V \frac{\Phi^{n+1} - \Phi^n}{\Delta t} + A = D + S \quad (4)$$

... (4) where,

- Φ is the advected variable
- A is the advection flux
- D is the diffusion flux
- S is the source flux

As demonstrated by Patankar [1], the application of a finite differencing approach leads to a checkerboard pressure field and a pressure-velocity decoupling. To solve this problem we use a pressure correction approach as suggested by Patankar [1].

The following numerical approach was adopted:

- 1) Generation of grid (max size 100 x 100) with cell clustering near the edges of the prism.
- 2) Calculation of advection, diffusion and source fluxes at each control volume.
- 3) Semi-explicit calculation of mass imbalance and subsequent application of the pressure correction method to refine values of velocity at each cell centre.
- 4) Iteration till continuity is obeyed.

2.2. Solver details

The semi-explicit method [2] was used for generating the model.

$$u_{i,j}^{n+1} = u_{i,j}^n + \frac{dt}{\rho dV} (D_{i,j}^n - A_{i,j}^n + (p_{i-1/2,j}^{n+1} - p_{i+1/2,j}^{n+1}) dy)$$

$$v_{i,j}^{n+1} = v_{i,j}^n + \frac{dt}{\rho dV} (D_{i,j}^n - A_{i,j}^n + (p_{i,j-1/2}^{n+1} - p_{i,j+1/2}^{n+1}) dx)$$

Predictor:

$$\begin{aligned} u_{i,j}^* &= u_{i,j}^n + \frac{dt}{\rho dV} (D_{i,j}^n - A_{i,j}^n + (p_{i-1/2,j}^n - p_{i+1/2,j}^n) dy) \\ v_{i,j}^* &= v_{i,j}^n + \frac{dt}{\rho dV} (D_{i,j}^n - A_{i,j}^n + (p_{i,j-1/2}^n - p_{i,j+1/2}^n) dx) \end{aligned}$$

Corrector:

$$\begin{aligned} u'_{i,j} &= \frac{dt}{\rho dV} ((p'_{i-1/2,j} - p'_{i+1/2,j}) dy) \\ v'_{i,j} &= \frac{dt}{\rho dV} ((p'_{i,j-1/2} - p'_{i,j+1/2}) dx) \end{aligned}$$

Pressure Correction Equation:

$$a_{i,j} (p'_{i,j}^{n+1} - p_{i,j}^n) = -(\sum_f F_f^{*n} + \sum_f F_f'^n)$$

Boundary Conditions:

No slip:

$$u = 0 ; \frac{\partial p}{\partial n} = \mu \frac{\partial^2 u}{\partial n^2}, \frac{\partial p'}{\partial n} = 0$$

Inlet:

$$u_n = u_{in}; u_t = 0; \frac{\partial p'}{\partial n} = 0$$

$$\frac{\partial p}{\partial n} = -\left(\frac{\partial(\rho u_n)}{\partial t} + \nabla \cdot (\rho uu_n) - \mu \nabla^2 u_n\right)$$

Free slip:

$$u_n = 0; \frac{\partial u_t}{\partial n} = 0; \frac{\partial p'}{\partial n} = 0$$

$$\frac{\partial p}{\partial n} = -\left(\frac{\partial(\rho u_n)}{\partial t} + \nabla \cdot (\rho uu_n) - \mu \nabla^2 u_n\right)$$

Outlet:

$$\frac{\partial u}{\partial n} = 0; \frac{\partial u}{\partial t} + U_c \frac{\partial u}{\partial n} = 0; p = 0; p' = 0$$

The following conditions were imposed while writing the code:

- The fluid is considered to be incompressible and hence $\rho = \text{constant}$.
- Effect of temperature on viscosity is neglected.
- Flow is subsonic and occurs at low values of Reynolds number.
- The orientation and structural integrity of the solid obstacle remain constant throughout the duration of the flow.
- The dimensional constraints are shown in the figure 1.

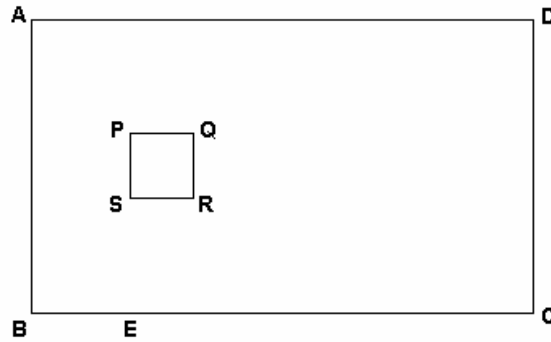


Figure 1. Dimensional constraints: $AB=CD=10$; $AD=BC=16$; $BE=3.125$; $PQ=QR=RS=SP=2$.

- The entire left boundary is an inlet boundary, with the right boundary being an exit boundary. The top and bottom boundaries are at free slip.
- The surfaces of the square prism are no slip edges.
- The Courant-Friedrich-Lowy and Grid Fourier Number criteria were used for determining the time step.
- The convergence criterion was set to a mass imbalance of 1×10^{-5} units.

3. Results and discussion

The model was developed at a kinematic viscosity of $0.01035 \text{ m}^2/\text{s}$ (say Fluid A) and then it was validated by comparing it with numerical models developed by Norberg [5, 6] and Robichaux [4] as shown below.

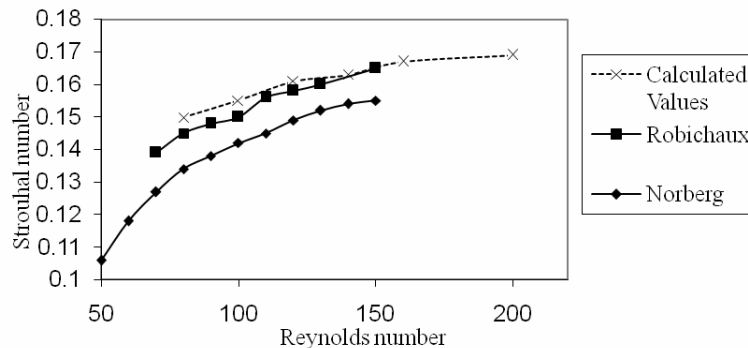
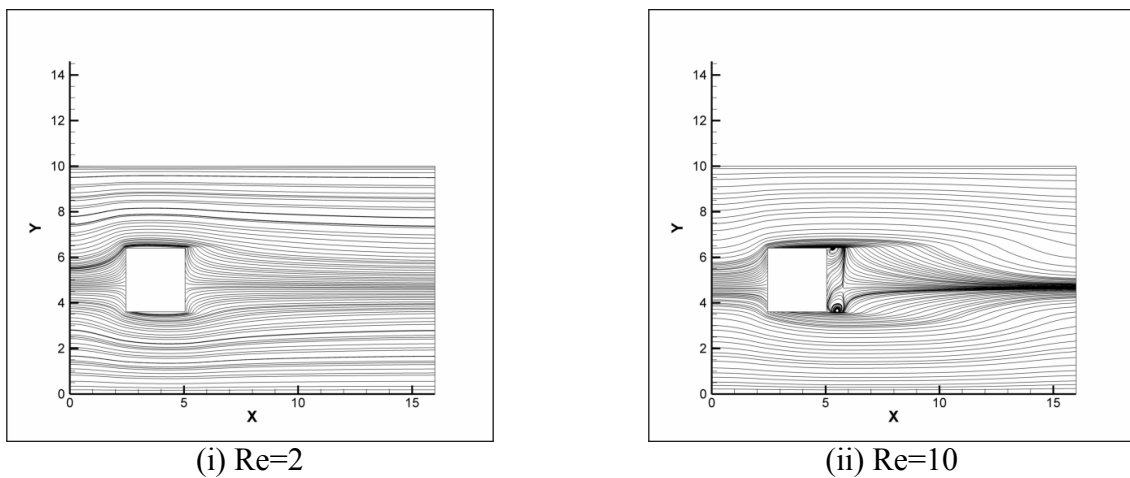


Figure 2. Variation of Strouhal number with Reynolds number

The following outputs were obtained on execution. The figures that follow show the variation in vortex shedding characteristics with increasing values of the Reynolds number for the oil.



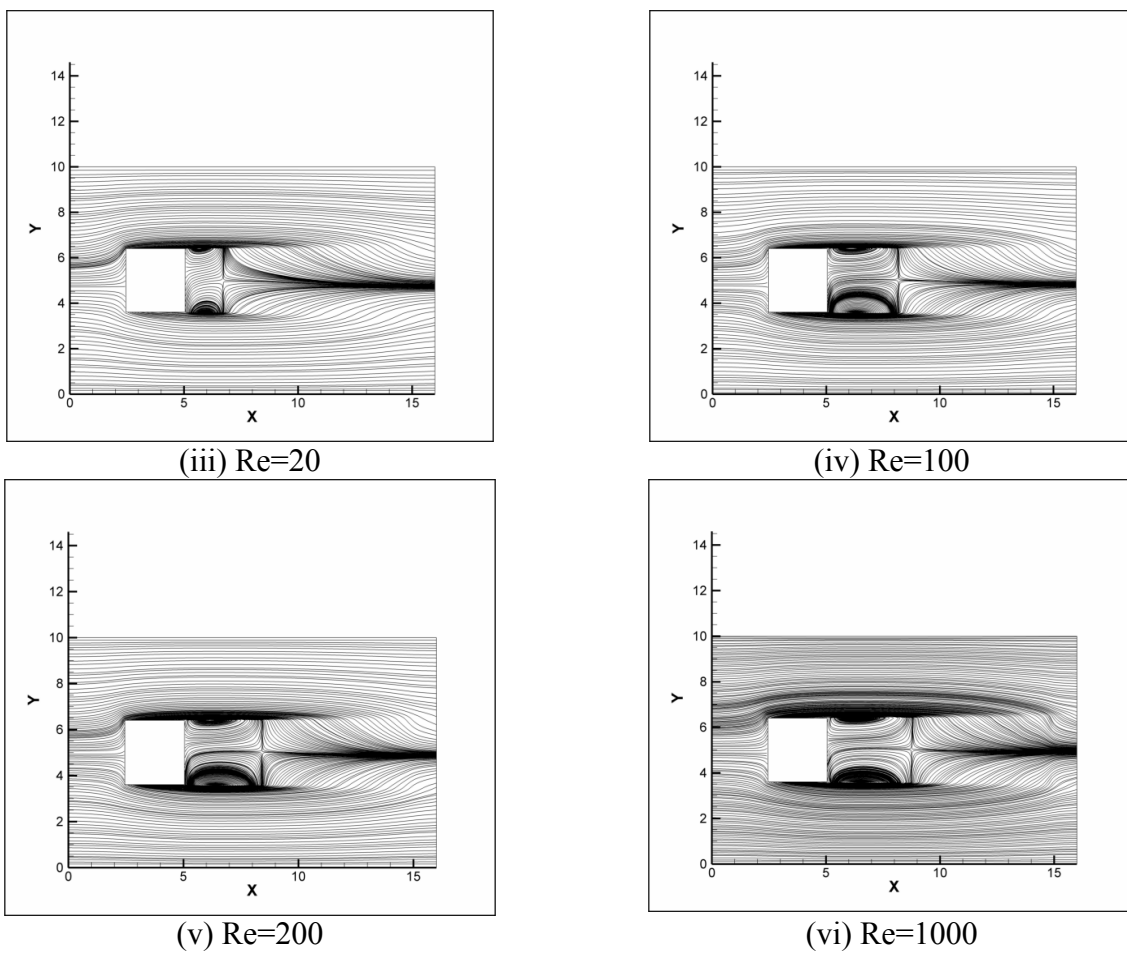
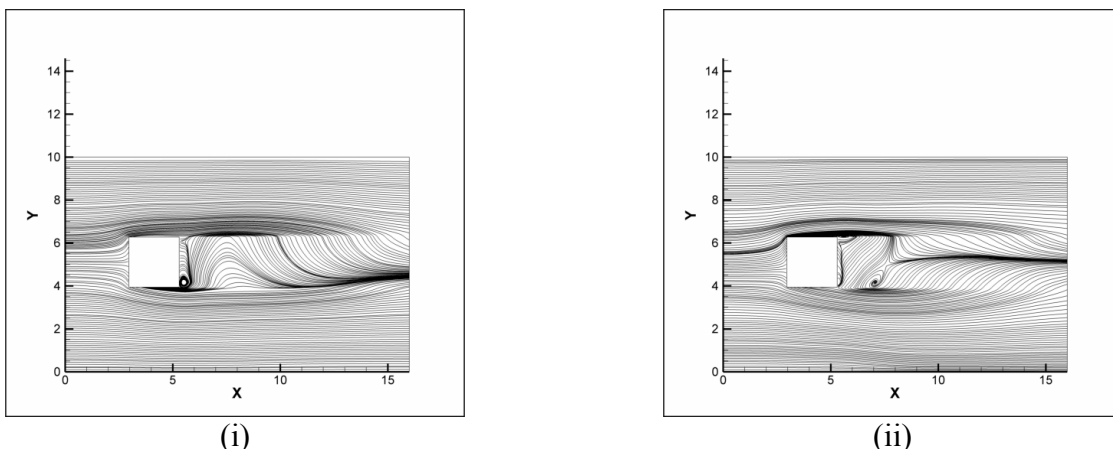


Figure 3. Nature of flow with increasing Reynolds Number for Fluid A

The above results shown in figure 3 are displayed at steady state. Initially, the flow is highly laminar and the flow does not show any separation. Eventually as the Reynolds number reaches $Re=100$, eddy formation begins on the downstream side. As Reynolds number reaches a critical value, flow separation begins and tendency of vortex formation increases. Thus, for high kinematic viscosity, the tendency of the fluid to stick to the no-slip surfaces increases. Hence, a clear flow separation does not occur till higher values of Reynolds number are attained.

Parallel to this, a study was carried out into the flow development characteristic of a low viscosity, low density fluid to demonstrate the vortex shedding phenomenon. This was done primarily with the aim of comparing the stages of flow development for fluids with different viscosities. For this purpose the kinematic viscosity was chosen to be $1.33 \times 10^{-5} \text{ m}^2/\text{s}$ (say Fluid B) which is considerably smaller than that of Fluid A.



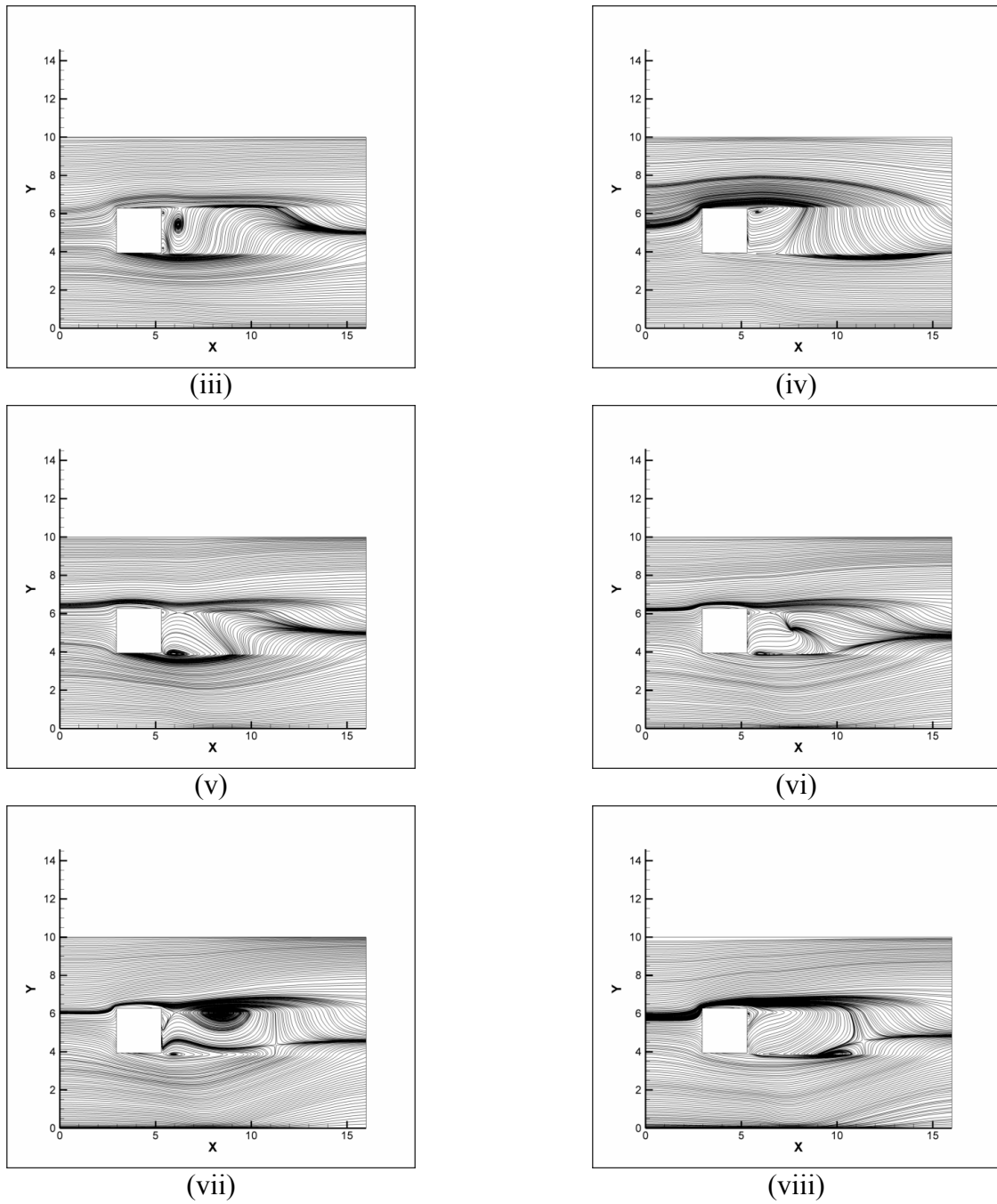


Figure 4. Development of flow at $\text{Re}=200$

The simulation was run at $\text{Re}=200$. The dimensions and orientation of the prism, and the mesh used were the same as those used in the previous study. The development of the vortex is shown in 8 stages. The alternate shedding on the top and the bottom of the prism is seen in the figure.

As seen in the figure 4, even at a low Reynolds Number, the vortex shedding is quite significant and the fluid particles have a greater tendency to separate from the solid surface. As a result, Fluid B shows vortex shedding much earlier than Fluid A. Consequently, we may infer that the vortex shedding tendency is largely dependent on the kinematic viscosity of the fluid under consideration.

4. Conclusion

From the above studies, we have concluded that the flow separation and vortex shedding phenomena are largely governed by the kinematic viscosities of the fluid even at the same value of the Reynolds number. Also, for a fluid, the shedding phenomenon occurs only beyond a critical value of the Reynolds number. Further investigations may be conducted into investigating such flows across obstacles of arbitrary shape to evaluate drag and lift characteristics across such obstacles.

Nomenclature

V	Resultant velocity
u	Velocity in X-direction
v	Velocity in Y-direction
u_n	Normal velocity
u_t	Tangential velocity
p	Pressure
σ	Normal Stress
τ	Shear Stress
ΔV	Volume
dt	Time step
ρ	Density
Re	Reynolds Number
F_f	Mass Flux
*	Predicted value of
,	Corrected value of
μ	Dynamic Viscosity

References

- [1] Patankar S. V. The Calculation of the Flow Field – The Simple Algorithm, Numerical Heat Transfer and Fluid Flow, Taylor and Francis Publishers 2005 p. 126-130
- [2] Sharma A. and Eswaran V. Finite Volume Method, Computational Fluid Flow and Heat Transfer, Narosa Publishing House, India 2008 p. 445-482
- [3] Anderson J. D. The Governing Equations of Fluid Dynamics, Computational Fluid Dynamics – The Basics with Applications, McGraw-Hill Inc. USA. 1995 p. 75-80
- [4] Robichaux J. Balachandar S. and Vanka S. P. Two-dimensional Floquet Instability of the Wake of Square Cylinder, Phys. Fluids, Vol. 11 1999 p. 560-578
- [5] Sohankar A. Norberg C. Davidson L., Numerical Simulation of Unsteady Low Reynolds Number Flow around Rectangular Cylinders at Incidence, J. Wind Engg. Ind. Aerodyn., Vol. 69 1997 p. 189-201
- [6] Sohankar A. Norberg C. Davidson L., Low Reynolds Number Flow around a Square Cylinder at Incidence: Study of Blockage, Onset of Vortex Shedding and Outlet Boundary Condition, Int. J. Num. Methods Fluids, Vol. 26 1998 p. 39-56